

## Self-avoiding walks on compact fractals: Exact and Monte Carlo renormalization-group results

Ivan Živić

*Faculty of Natural Sciences and Mathematics, The Svetozar Marković University,  
34000 Kragujevac, Serbia, Yugoslavia*

Sava Milošević

*Faculty of Physics, University of Belgrade, P.O. Box 550, 11001 Belgrade, Serbia, Yugoslavia*

H. Eugene Stanley

*Center for Polymer Studies and Department of Physics, Boston University, Boston, Massachusetts 02215*

(Received 5 October 1992)

We present an exact and Monte Carlo renormalization-group (MCRG) study of the self-avoiding walks (SAW's) on an infinite family of the plane-filling (PF) fractals. The fractals are compact, that is, their fractal dimension  $d_f$  is equal to 2 for all values of the fractal enumerator  $b$  (an odd integer,  $3 \leq b < \infty$ ). On the other hand, we demonstrate, via precise calculations, that the corresponding spectral dimension  $d_s$  monotonically increases from 1.39385 to 2, when  $b$  varies from 3 to  $\infty$ . For the PF fractals, we calculate exactly (for  $3 \leq b \leq 9$ ) and through the MCRG approach (for  $b \leq 121$ ) the SAW critical exponents  $\nu$  (associated with the mean-squared end-to-end distance) and  $\gamma$  (associated with the total number of distinct SAW's). The MCRG results for  $3 \leq b \leq 9$  deviate from exact results at most 0.04% in the case of  $\nu$  and 0.06% in the case of  $\gamma$ . Our results show clearly that  $\nu$  monotonically decreases with  $b$  and crosses the Euclidean value  $\nu = 3/4$  between  $b = 27$  and  $b = 29$ . This is in contrast with all available Flory-type theories, as they predict that  $\nu$  should be, in the case under study, strictly less than  $3/4$ . In addition, our results show that the critical exponent  $\gamma$ , being always larger than the Euclidean value  $43/32$ , monotonically increases with  $b$ . We discuss, in a framework of the finite-size scaling approach, behavior of  $\nu$  and  $\gamma$  in the fractal-to-Euclidean crossover region that occurs when  $b \rightarrow \infty$ . Finally, we discuss a possible relevance of our results to the problem of SAW's on the two-dimensional percolation clusters.

PACS number(s): 05.40.+j, 05.50+q, 64.60.Ak, 61.41.+e

### I. INTRODUCTION

The self-avoiding walk (SAW) is a random walk that must not contain self-intersections. The influence of quenched imperfections of the underlying lattice on the statistics of SAW's has become a controversial research problem in the past decade. Various kinds of imperfections that perturb the translational symmetry of the underlying lattice have been introduced in order to learn their influence on the critical exponents of SAW's. In particular, the case of lattices randomly perturbed to the extent of being close to the percolation threshold has been most frequently studied. The problem is relevant to the phenomenology of linear-chain polymers in the dilute solution confined in a porous media. Various theoretical methods have been applied, including the exact enumerations, the Flory-type approximations, the Monte Carlo (MC) simulations, and the renormalization group (RG) techniques (see, for instance, Refs. [1-4], and references quoted therein). Simply speaking, in spite of numerous studies, it is not yet known whether the SAW walker, which on a perturbed lattice has to avoid both previously visited sites and lattice imperfections, travels (on average) farther away from the starting point than a SAW walker on an unperturbed lattice. In other words, it is not yet known whether in the relation  $\langle R_N^2 \rangle \sim N^{2\nu}$ , for

the mean-squared end-to-end distance for  $N$ -step SAW's, the critical exponent  $\nu$  changes when the underlying lattice gets perturbed. Thus, in the case of SAW's on the two-dimensional percolating clusters it is not firmly established hitherto whether  $\nu$  is larger than, or equal to, the Euclidean value  $3/4$  [5]. Under these circumstances, knowledge of exact properties of SAW's on infinite families of nontrivial deterministic fractals, which in a certain limit approach a standard Euclidean lattice, should provide grounds for systematic tests of various approximate studies.

In this paper we report on the exact and the Monte Carlo renormalization-group (MCRG) study of SAW's on an infinite family of fractals that can be considered as self-similarly perturbed two-dimensional square lattices (with various degrees of inhomogeneity). More specifically, we study SAW's on the plane-filling (PF) fractal lattices [6] and demonstrate that the corresponding exponent  $\nu$  can be larger, as well as smaller, than  $3/4$ . This result challenges further phenomenological investigations since all available Flory-type formulas [7-12] for  $\nu$  erroneously predict that it should be, in the case under study, strictly less than  $3/4$ .

The failure of the phenomenological formulas [7-12] to fit sequences of the exact (and MCRG) results for the SAW critical exponents for infinite families of deter-

ministic fractals has been already observed in the case of the Sierpinski gasket (SG) family of fractals [13,14] and, recently, in the case of two newly introduced families of deterministic fractals [15]. Here we notice that all phenomenological formulas are certain algebraic combinations of the fractal  $d_f$  and spectral  $d_s$  dimensions of the relevant fractals, which, in the case of fractals studied, appears to be a plausible choice of a minimal set of parameters. However, one may question which of the two parameters ( $d_f$  or  $d_s$ ) predominantly determines the behavior of the SAW critical exponents. The study of SAW's on the PF family of fractals provides an inspiring answer to this question, for in this case the fractal dimension is constant ( $d_f = 2$  for all members of this family), whereas  $d_s$  monotonically increase from 1.393 85 to 2 when the fractal enumerator  $b$  (the positive odd integer) varies from 3 to infinity. Nevertheless, our results show that the SAW critical exponent  $\nu$  has the same intriguing behavior that was found for the SG family [14], whose both  $d_f$  and  $d_s$  monotonically approach the Euclidean value of 2 from below when the fractal enumerator  $b$  (the positive integer,  $b \geq 2$  in this case) tends to infinity. This finding suggests that the future quests for closed-form formulas for the critical exponents of SAW's on fractal lattices should give a stronger emphasis on the role of the spectral dimension.

The present paper is organized as follows. We define the PF family of fractals in Sec. II, where we also present calculation of the corresponding spectral dimensions. In Sec. III, we explain our exact and MCRG approach to the evaluation of the critical exponents  $\nu$  and  $\gamma$  of SAW's on the PF fractals. Finally, in Sec. IV we present an overall discussion of the obtained results and pertinent conclusions.

## II. PLANE-FILLING FRACTAL LATTICES

Each member of the PF fractal family is labeled by an odd integer  $b$  ( $3 \leq b < \infty$ ) and can be constructed in stages. At the initial stage ( $n = 1$ ), the lattice is represented by the corresponding generator (see Fig. 1). The  $n$ th stage fractal structure can be obtained in a self-similar way, that is, by enlarging the generator by a factor  $b^{n-1}$  and by replacing each of its segments with the  $(n - 1)$ th stage structure, so that the complete fractal is obtained in the limit  $n \rightarrow \infty$ . The shape of the fractal generators and the way the fractals are constructed imply that each member of the family has the fractal di-

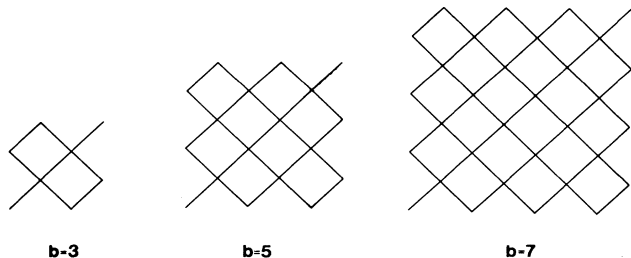


FIG. 1. The fractal generators of the first three members of the plane-filling (PF) family of fractals.

mension  $d_f$  equal to 2. Thus, they appear to be compact objects (with no voids) embedded in the two-dimensional Euclidean space. In fact, the PF fractals mimic imperfect square lattices with various degrees of inhomogeneity distributed self-similarly. In Fig. 2, the  $n = 2$  stage of the  $b = 5$  fractal is depicted and one can see that appearance of a lattice imperfection is equivalent to the elimination of the corresponding site together with binding two pairs of the remaining bonds.

The spectral dimension  $d_s$  of the PF fractals can be obtained by studying some dynamical problem related to the fractal substrata. We have found that it is useful to conceive an arbitrary member of the PF family as an electrical network of unit resistors corresponding to the segments of unit length (see, for instance, Refs. [16,17]). Then the spectral dimension is given by

$$d_s = \frac{4}{2 + \zeta}, \quad (2.1)$$

where  $\zeta$  is the exponent of the scaling law  $R_L \propto L^\zeta$  which governs the resistance  $R_L$  of the fractal structure of size  $L$ . This scaling law implies the following relation:

$$\zeta = \ln R_b / \ln b, \quad (2.2)$$

where  $R_b$  is the electrical resistance of the fractal generator.  $R_b$  can be calculated straightforwardly [6] up to, say,  $b = 11$ , when the problem becomes too complex and one has to apply a computer facility. For an arbitrary member of the PF family with  $b > 3$ , a computer program can be made to calculate  $R_b$ , by evaluating the electrical currents through the fractal bonds in accord with Kirchhoff's laws and the underlying axial symmetry of the fractal generator. Eventually, it turns out that one has to solve  $(b - 3)/2$  linear nonhomogeneous equations with very high precision [18].

The results obtained for  $R_b$  and  $d_s$  are given in Table I. In order to learn the asymptotic behavior  $d_s$  we have plotted (following the approach of Ref. [17]) data for  $R_b$  versus  $\ln b$  (see Fig. 3). One can observe that all

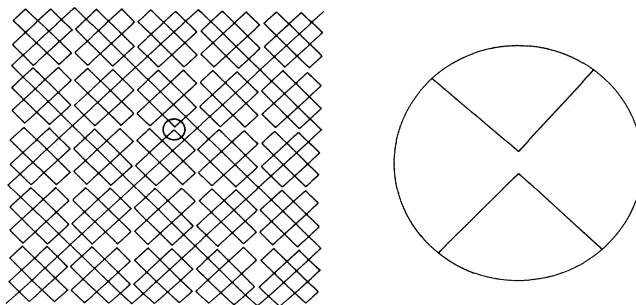


FIG. 2. The  $n = 2$  stage fractal structure of the  $b = 5$  member of the PF family of fractals. It should be noted that this structure looks like a square lattice with imperfections. Indeed, the complete fractal structure (that appears in the limit  $n \rightarrow \infty$ ) has no voids. It has self-similarly distributed imperfections of the type exemplified within the small circle. In the large circle, a lattice imperfection is blown up (the two tips would be merged into a single lattice site, in the case of an unperturbed square lattice).

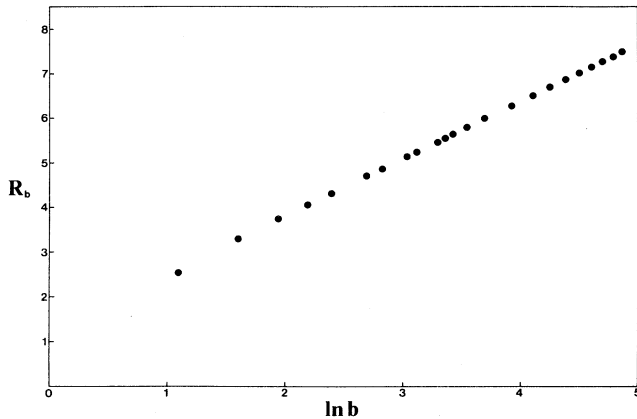


FIG. 3. Data for the electrical resistance  $R_b$  (of the fractal generators) plotted against  $\ln b$ . One can see that all data (except those for small  $b$ ) comprise a straight line. The least-squares fit to the data is given by Eq. (2.3).

data for  $R_b$  display remarkable linear dependence of  $\ln b$ . Indeed, the least-squares fit to a linear function of  $\ln b$  demonstrates that the mean-square deviations, including all data, is not larger than  $10^{-4}$ , whereas in the case when the data for  $b < 35$  are excluded one finds that the deviations are not larger than  $10^{-9}$ . Therefore, we have concluded that  $R_b$  can be represented in the form

$$R_b = 1.273 \ln b + 1.271, \tag{2.3}$$

where the quoted numbers remain unchanged for any least-squares fit that starts with some  $b \geq 35$  and ends with  $b = 131$ . The above conclusion, together with formulas (2.1) and (2.2), implies the following asymptotic law for the PF fractal spectral dimension:

$$d_s = 2 - \frac{\ln \ln b}{\ln b}, \tag{2.4}$$

which is valid in the fractal to Euclidean crossover region, that is, for very large  $b$ . It is interesting to observe that the asymptotic form of the type (2.4) has been also established in the case of the SG family of fractals [17,19].

TABLE I. The electrical resistance  $R_b$  of the PF fractal generators and the corresponding spectral dimensions  $d_s$ .

$b$	$R_b$	$d_s$	$b$	$R_b$	$d_s$
3	2.60000	1.39385	35	5.79904	1.60360
5	3.29885	1.45900	41	6.00062	1.61127
7	3.73903	1.49380	51	6.27862	1.62124
9	4.06356	1.51624	61	6.50665	1.62894
11	4.32131	1.53236	71	6.69997	1.63517
15	4.71828	1.55467	81	6.86777	1.64037
17	4.87818	1.56289	91	7.01601	1.64481
21	5.14786	1.57592	101	7.14877	1.64867
23	5.26389	1.58122	111	7.26898	1.65208
27	5.46833	1.59015	121	7.37882	1.65512
29	5.55941	1.59397	131	7.47993	1.65786
31	5.64440	1.59746			

However, in what follows, this similarity between the two families of fractals should be kept in mind together with the basic difference between the corresponding fractal dimensions ( $d_f = 2$  for each  $b$ , in the PF case, whereas  $d_f = \ln[b(b + 1)/2]/\ln b$  in the SG case).

### III. EXACT AND MONTE CARLO RENORMALIZATION-GROUP CALCULATION OF THE CRITICAL EXPONENTS

In this section we determine the critical exponents  $\nu$  and  $\gamma$  of SAW's on the PF family of fractals. The critical exponent  $\nu$  describes the scaling law  $\langle R_N^2 \rangle \sim N^{2\nu}$  for the mean-squared end-to-end distance for  $N$ -step SAW's, whereas the critical exponent  $\gamma$  determines the scaling law  $C_N \sim \mu^N N^{\gamma-1}$  for the total number  $C_N$  of distinct SAW's of  $N$  steps (averaged over all possible positions of the starting point). Here  $\mu$  is the connectivity constant, and it is assumed that  $N$  is a very large number. These critical exponents we calculate in the framework of the RG method, in which we study the corresponding generating functions that can be defined by introducing the weight factor  $x$  (fugacity) for each step of SAW. Thus, we first recall the generating functions  $C(x)$  and  $L(x)$  defined by

$$C(x) = \sum_{N=1}^{\infty} C_N x^N, \tag{3.1}$$

$$L(x) = \sum_{N=2}^{\infty} \langle R_N^2 \rangle C_N x^N / C(x), \tag{3.2}$$

whose leading singular terms, when  $x$  approaches  $1/\mu$  from below, are of the form

$$C(x) \sim (1 - x\mu)^{-\gamma}, \tag{3.3}$$

$$L(x) \sim (1 - x\mu)^{-2\nu}. \tag{3.4}$$

In order to calculate  $\nu$  and  $\gamma$  we have found that it is convenient to introduce three restricted partition functions  $A^{(n)}$ ,  $B^{(n)}$ , and  $C^{(n)}$  (see Fig. 4) which provide a com-

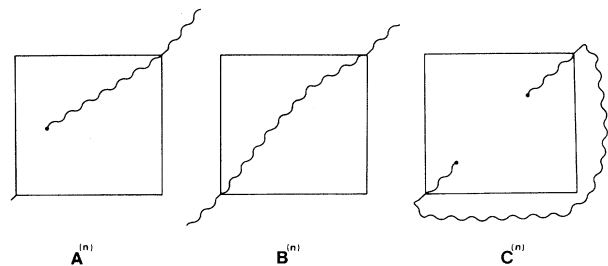


FIG. 4. A diagrammatic representation of the three restricted partition functions for an  $n$ th stage of the fractal construction of a member of the PF family. The fractal interior structure is not shown. Thus, for example,  $A^{(n)}$  represents the SAW path that starts somewhere within the  $n$ th stage fractal structure and leaves it at its upper right link to rest of fractal.

plete description of the appropriate generating functions  $C(x)$  and  $L(x)$  [15,20]. The three restricted partition functions represent sums of statistical weights of all possible walks within the  $n$ th-stage fractal structure for the three kinds of SAW's that are consistent with the constraints depicted in Fig. 4. Thus,  $A^{(n)}$  is the weighted sum over all walks that start somewhere within the  $n$ th-stage fractal structure and leave it at its upper right link to the rest of fractal, whereas  $B^{(n)}$  is the weighted sum of all walks that start at the lower left link of the  $n$ th-stage fractal structure and leave it at its upper right link, and, finally,  $C^{(n)}$  is the weighted sum of all walks that start and end at two locations within the  $n$ th-stage fractal structure (see Fig. 4). In the case of the fractal unit segment, we accept the following initial conditions for the three restricted partition functions

$$A^{(0)} = \sqrt{x}, \quad B^{(0)} = x, \quad C^{(0)} = 0. \quad (3.5)$$

For arbitrary  $n$ , the self-similarity of the fractals under study imply the following recursion relations:

$$A^{(n)} = \psi_1(A^{(n-1)}, B^{(n-1)}), \quad (3.6)$$

$$B^{(n)} = \psi_2(B^{(n-1)}), \quad (3.7)$$

$$C^{(n)} = \psi_3(A^{(n-1)}, B^{(n-1)}, C^{(n-1)}). \quad (3.8)$$

Equation (3.6), for instance, states the fact that a walk of the type  $A$  (see Fig. 4), within the  $n$ th-stage fractal structure, can be composed only of a walk of the type  $A$  and walks of the type  $B$  performed within the next smaller structures, that is, of the  $A$  and  $B$  (but no  $C$ ) walks within the  $(n-1)$ th fractal structures. The explicit forms of the functions  $\psi_1$ ,  $\psi_2$ , and  $\psi_3$  are, because of the underlying self-similarity, independent of the specific value of  $n$ , which allows one to state that the three equations (3.6), (3.7), and (3.8), comprise the exact renormalization group for the SAW problem under study.

#### A. Critical exponent $\nu$

We apply in this subsection the foregoing RG framework to find the SAW critical exponent  $\nu$  for the PF fractals. We shall first present the corresponding exact calculation, and then we shall expound on the MCRG approach. To this end, we need to analyze (3.7), at the corresponding fixed point, for  $B^{(1)}$  and  $B^{(0)}$  denoted by  $x'$  and  $x$ , respectively. It can be shown that  $\psi_2(x)$  is a simple polynomial

$$x' = \sum_N a_N x^N, \quad (3.9)$$

whose first term is of the order  $x^b$ . The coefficients  $a_N$  are numbers of all possible SAW's of  $N$  steps that traverse the fractal generator. Specific values of the critical exponent  $\nu$  follows from

$$\nu = \frac{\ln b}{\ln \lambda_1}, \quad (3.10)$$

where  $\lambda_1$  is the relevant eigenvalue of the RG equation

(3.9) at the nontrivial fixed point  $0 < x^* < 1$  (see, for instance, [13] and [20]), that is

$$\lambda_1 = \left. \frac{dx'}{dx} \right|_{x^*}. \quad (3.11)$$

Accordingly, evaluation of  $\nu$  starts with determining the coefficients  $a_N$  of (3.9) and finding of the pertinent fixed point value  $x^*$ . We have been able to find exact values of  $a_N$  for  $3 \leq b \leq 9$  (these values are given in the Appendix; calculation of exact values of  $a_N$  for  $b = 11$  would require more than 100 days of continuous work of a computer with the Intel 80486 microprocessor). Knowing  $a_N$  and  $x^*$ , for a given  $b$ , we apply (3.10) and (3.11) to learn the critical exponent  $\nu$ . Our results are presented in Table II.

To overcome the computational problem of learning exact values of  $a_N$ , we apply the MCRG method for  $b > 9$ . It has been pointed out in a similar situation [14] that, due to both the inherent self-similarity and the finite ramification of the underlying lattices, this method should work better in this case than in the case of regular lattices. The essence of the MCRG method [14,21] consists of treating  $x'$ , given by (3.9), as the grand canonical partition function which comprises all possible SAW's that traverse the fractal generator at two fixed apexes. In this spirit, (3.9) allows us to write the following relation:

$$\frac{dx'}{dx} = \frac{x'}{x} \langle N(x) \rangle, \quad (3.12)$$

where  $\langle N(x) \rangle$  is given by

$$\langle N(x) \rangle = \frac{1}{x'} \sum_N N a_N x^N, \quad (3.13)$$

which can be considered as the average number of the SAW steps, made at fugacity  $x$  by all possible SAW's that pass the fractal generator. Comparing (3.11) with (3.12) we obtain the equality  $\lambda_1 = \langle N(x^*) \rangle$ , and thereby we obtain

$$\nu = \frac{\ln b}{\ln \langle N(x^*) \rangle}. \quad (3.14)$$

This is the formula that enables us to calculate  $\nu$  via the constant-fugacity MCRG method [22], that is, without calculating explicitly the coefficients  $a_N$ .

In this paragraph we present the MCRG algorithm of finding the critical fugacity  $x^*$ . The algorithm starts with the MC simulation for a given initial guess for the fugacity  $x_0$  in the region  $0 < x_0 < 1$ . Here  $x_0$  can be interpreted as the probability of making the next step along an available direction from the vertex that the SAW walker has reached. Then we assume that, after the experiment is completed, we have  $S_0$  total number of the MC simulations of SAW's (at the chosen  $x_0$ ), with  $S_0^t$  of them being those that traverse the fractal generator. Hence the ratio  $S_0^t/S_0$  can be accepted as the renormalized fugacity  $x'_0$  of the coarse-grained fractal structure. In this way we get the value of the sum (3.9) without specifying the set  $a_N$ . The next (closer to  $x^*$ ) values  $x_m$  ( $m \geq 1$ ), at which the MC simulation should be performed, can be found by using the "homing" procedure [22], which can be ter-

minated at the stage  $m$  when the difference  $x_{m+1} - x_m$  becomes less than the statistical uncertainty associated with  $x_m$ . Consequently,  $x^*$  can be identified with the last value  $x_{m+1}$  found in this way.

Having found  $x^*$  we can evaluate  $\langle N(x^*) \rangle$  using the following expansion formula

$$\langle N(x^*) \rangle = \langle N(x_m) \rangle + \frac{x^* - x_m}{x_m} \mathcal{D}(N(x_m)), \quad (3.15)$$

where  $\mathcal{D}(N) = \langle N^2 \rangle - \langle N \rangle^2$  is the fluctuation of the number  $N$  of SAW steps (measured at  $x = x_m$ ). The quantities that appear on the right-hand side of (3.15),  $\langle N(x_m) \rangle$  and  $\mathcal{D}(N(x_m))$ , can be determined *directly* through the MC simulations, which means that we have all elements necessary to calculate  $\nu$  using (3.14). In Table II we present our MCRG results for  $\nu$  for the PF fractal lattices with  $b \leq 121$ . First, we note that comparing the MCRG results for  $3 \leq b \leq 9$  with the exact results we can see that there is no deviation larger than 0.04%. Next, we would like to point out the monotonic decrease of  $\nu$  when  $b$  increases, and, in particular, the crossing of the Euclidean value  $\nu = 0.75$  between  $b = 27$  and  $b = 29$ . This crossing of the Euclidean value should be compared with the similar crossing found [14] in the case of the

SG family of fractals. The results for both families are depicted in Fig. 5, where one can see that the two cases display amazingly similar behavior (for  $b > 3$ ) in spite of the fact that the corresponding fractal dimensions are quite disparate functions of  $b$ . The possibility that  $\nu$  will regain the Euclidean value  $\nu = 3/4$  in the crossover region  $b \rightarrow \infty$ , and an overall comparison with the phenomenological predictions for  $\nu$ , will be discussed in Sec. IV.

## B. Critical exponent $\gamma$

The critical exponent  $\gamma$  describes the scaling law  $C_N \sim \mu^N N^{\gamma-1}$  for the total number  $C_N$  of distinct SAW's of  $N$  steps, and thereby it determines the singular part (3.3) of the generating function  $C(x)$  defined by (3.1). In order to determine  $\gamma$  as a function of the fractal enumerator  $b$ , we first note that, in the case of the PF family,  $C(x)$  can be written in the form

$$C(x) = \sum_{n=1}^{\infty} \frac{1}{b^{2n}} \{g_1(B^{(n-1)})[A^{(n-1)}]^2 + g_2(B^{(n-1)})[C^{(n-1)}]\}, \quad (3.16)$$

TABLE II. The exact ( $3 \leq b \leq 9$ ) and the MCRG ( $3 \leq b \leq 121$ ) results for the critical fugacity  $x^*$ , the RG eigenvalue  $\lambda_1$ , and the SAW critical exponent  $\nu$ . The given error bars have been determined by statistics of the MC simulations and by the "homing" procedure used in evaluation of  $x^*$  and  $\lambda_1$  [22]. The extrapolation of the least-square fits of the  $x^*$  data gives  $x^* = 0.37931$  for  $b \rightarrow \infty$ , which deviates 0.07% from the reciprocal of the connectivity constant  $\mu = 2.638159$  found for the standard square lattice [23].

$b$	No MC realization	$x^*$	$\lambda_1$	$\nu$
3	exact	0.70711		0.79248
	$2 \times 10^5$	$0.70734 \pm 0.00045$	$3.999 \pm 0.003$	$0.79259 \pm 0.00038$
5	exact	0.59051		0.78996
	$2 \times 10^5$	$0.59060 \pm 0.0032$	$7.667 \pm 0.005$	$0.79011 \pm 0.00024$
7	exact	0.53352		0.78111
	$10^5$	$0.53351 \pm 0.00034$	$12.08 \pm 0.01$	$0.78102 \pm 0.00031$
9	exact	0.50029		0.77464
	$10^5$	$0.50039 \pm 0.00027$	$17.06 \pm 0.02$	$0.77459 \pm 0.00029$
11	$2 \times 10^5$	$0.47832 \pm 0.00016$	$22.56 \pm 0.02$	$0.76947 \pm 0.00019$
15	$2 \times 10^5$	$0.45191 \pm 0.00013$	$34.90 \pm 0.03$	$0.76232 \pm 0.00017$
17	$2 \times 10^5$	$0.44321 \pm 0.00011$	$41.64 \pm 0.03$	$0.75976 \pm 0.00017$
21	$2 \times 10^5$	$0.43065 \pm 0.00010$	$56.33 \pm 0.05$	$0.75522 \pm 0.00016$
23	$2 \times 10^5$	$0.42593 \pm 0.00009$	$64.33 \pm 0.06$	$0.75300 \pm 0.00015$
27	$2 \times 10^5$	$0.41855 \pm 0.00008$	$80.49 \pm 0.07$	$0.75108 \pm 0.00015$
29	$5 \times 10^5$	$0.41573 \pm 0.00005$	$89.60 \pm 0.05$	$0.74905 \pm 0.00009$
31	$3 \times 10^5$	$0.41323 \pm 0.00006$	$98.45 \pm 0.07$	$0.74822 \pm 0.00012$
35	$2 \times 10^5$	$0.40913 \pm 0.00006$	$108.0 \pm 0.1$	$0.74530 \pm 0.00014$
41	$5 \times 10^5$	$0.40429 \pm 0.00004$	$148.39 \pm 0.08$	$0.74274 \pm 0.00008$
51	$10^5$	$0.39893 \pm 0.00007$	$203.5 \pm 0.3$	$0.73969 \pm 0.00017$
61	$10^5$	$0.39524 \pm 0.00006$	$265.6 \pm 0.3$	$0.73643 \pm 0.00017$
71	$10^5$	$0.39273 \pm 0.00006$	$329.8 \pm 0.4$	$0.73513 \pm 0.00016$
81	$10^5$	$0.39081 \pm 0.00005$	$401.0 \pm 0.5$	$0.73314 \pm 0.00015$
91	$10^5$	$0.38931 \pm 0.00005$	$474.1 \pm 0.6$	$0.73212 \pm 0.00014$
101	$3 \times 10^5$	$0.38812 \pm 0.00004$	$552.0 \pm 0.4$	$0.73098 \pm 0.00008$
111	$1.2 \times 10^5$	$0.38726 \pm 0.00004$	$631.7 \pm 0.7$	$0.73034 \pm 0.00013$
121	$10^5$	$0.38649 \pm 0.00004$	$721.8 \pm 0.8$	$0.72865 \pm 0.00013$

where  $g_1(B^{(n-1)})$  and  $g_2(B^{(n-1)})$  are polynomials in  $B^{(n-1)}$ . This form for  $C(x)$  stems from the fact that all possible open SAW's paths, within the  $n$ th-stage fractal structure, can be made in only two ways (see Fig. 6). Hence one can see that the behavior of  $C(x)$  in the vicinity of  $x^*$  depends on the corresponding behavior of the restricted partition functions  $A^{(n)}$ ,  $B^{(n)}$ , and  $C^{(n)}$ . Since in the preceding subsection we have learned the behavior of  $B^{(n)}(x)$ , it remains to analyze here the recursion relations (3.6) and (3.8). The structure of possible SAW paths (see Fig. 4) imply the following structure of the recursion relations:

$$A^{(n)} = a(B^{(n-1)})A^{(n-1)}, \quad (3.17)$$

$$C^{(n)} = c_1(B^{(n-1)})C^{(n-1)} + c_2(B^{(n-1)})[A^{(n-1)}]^2, \quad (3.18)$$

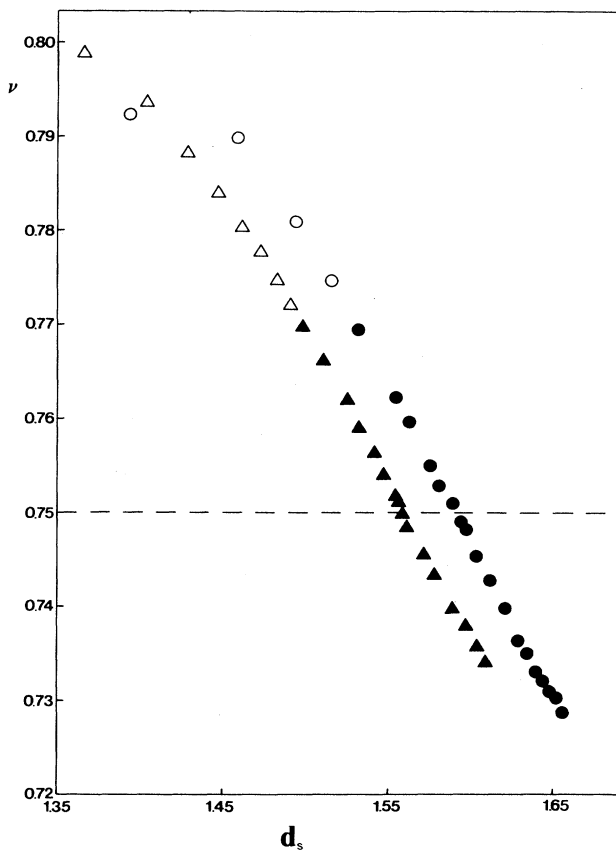


FIG. 5. Data for the SAW critical exponent  $\nu$  for the SG (triangles) and PF (circles) families of fractals plotted as functions of the corresponding spectral dimensions  $d_s$ . The open triangles (open circles) are exact results, while the solid triangles (solid circles) are the MCRG results. The error bars related to the MCRG data are not depicted in the figure since they are at least two times smaller than the heights (diameters) of the solid triangles (circles). The horizontal dashed line represents the Euclidean value  $\nu = 3/4$ . One should notice the remarkable similarity between the two sets of data (SG and PF) and recall the fact that the PF fractals are compact objects, in contrast to the SG fractals that have voids on all scales of length.

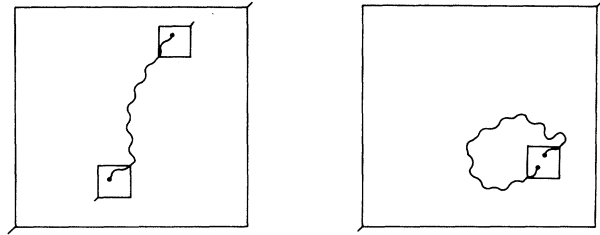


FIG. 6. The form of the generating function  $C(x)$  given by Eq. (3.16) stems from the fact that all possible open SAW's paths, within the  $n$ th stage fractal structure, can be made in only two ways that are depicted in this figure.

where  $a(B^{(n-1)})$ ,  $c_1(B^{(n-1)})$ , and  $c_2(B^{(n-1)})$  are also polynomials in  $B^{(n-1)}$ .

The above set of formulas allow us to find the critical exponent  $\gamma$ . To this end, we first note that, according to the procedure detailed in previous papers [13,20,24],  $\gamma$  can be expressed, in the case under study, in the following form:

$$\gamma = 2 \frac{\ln(\lambda_2/b)}{\ln \lambda_1}, \quad (3.19)$$

where  $\lambda_2$  is the RG eigenvalue

$$\lambda_2 = a(x^*) \quad (3.20)$$

of the polynomial  $a(B^{(n-1)})$  defined by (3.17), with  $x^*$  being the fixed point value of (3.9). Therefore, it remains either to find means to determine exactly an explicit expression for the polynomial  $a(B^{(n-1)})$  or to surpass this step and to evaluate somehow only the single value needed  $a(x^*)$ . We have been able to determine the exact form of the requisite polynomial for the PF fractals with  $3 \leq b \leq 9$ , while for  $b > 9$  we have applied the MCRG to evaluate  $a(x^*)$ .

In order to learn an explicit expression of the polynomial  $a(B^{(n-1)})$ , we note that its form, due to the underlying self-similarity, should not depend on  $n$ , and, for this reason, in what follows we assume  $n = 1$ . Then, one can verify the following expression:

$$a(x) = 1 + \sum_N Q_N x^N, \quad (3.21)$$

where  $Q_N$  is the number of all SAW's of  $N$  steps that start at any bond within the generator ( $n = 1$ ) and leaves it at a fixed exit, which implies that the above sum starts with the  $N = 1$  term. By enumeration of all relevant walks, the coefficients  $Q_N$  can be evaluated exactly up to certain finite  $b$ . In the Appendix we present specific values of  $Q_N$  for  $3 \leq b \leq 9$  (for larger  $b$  one would need more of the computer power than in the case of exact calculation of  $\nu$ ). Using the information given in the Appendix, together with (3.19) and (3.21) (and previously found  $x^*$  and  $\lambda_1$ ), we have obtained the desired values of  $\gamma$  (see Table III).

For  $b > 9$ , we extend the MCRG method, used in the preceding subsection, and in the similar spirit we conceive  $a(x)$  as a new grand canonical partition function defined

by (3.21). Its specific value  $a(x^*)$  we calculate using the expansion formula

$$a(x^*) = a(x_m) + \left. \frac{da(x)}{dx} \right|_{x_m} (x^* - x_m) + \frac{1}{2} \left. \frac{d^2a(x)}{dx^2} \right|_{x_m} (x^* - x_m)^2, \quad (3.22)$$

where  $a(x_m)$  is the quantity that can be directly measured in the MC simulations (in a manner exploited to measure  $x'$ ), whereas the derivatives

$$\frac{da(x)}{dx} = \sum_N N Q_N x^{N-1} \quad (3.23)$$

and

$$\frac{d^2a(x)}{dx^2} = \sum_N N(N-1) Q_N x^{N-2} \quad (3.24)$$

can be expressed in terms of the averages

$$\langle N(x) \rangle = \frac{1}{a(x)} \sum_N N Q_N x^N, \quad (3.25)$$

$$\langle N(x)^2 \rangle = \frac{1}{a(x)} \sum_N N^2 Q_N x^N, \quad (3.26)$$

TABLE III. The exact ( $3 \leq b \leq 9$ ) and the MCRG ( $3 \leq b \leq 121$ ) results for the RG eigenvalue  $\lambda_2$  and the SAW critical exponent  $\gamma$ . The given error bars are determined in the same way as in the case of data quoted in Table II.

b	No MC realization	$\lambda_2$	$\gamma$
3	exact		1.6840
	$5 \times 10^5$	$9.64 \pm 0.01$	$1.6840 \pm 0.0022$
5	exact		1.7423
	$5 \times 10^5$	$29.50 \pm 0.05$	$1.7419 \pm 0.0024$
7	exact		1.7614
	$5 \times 10^5$	$62.9 \pm 0.2$	$1.7625 \pm 0.0028$
9	exact		1.7807
	$5 \times 10^5$	$112.4 \pm 0.4$	$1.7803 \pm 0.0030$
11	$10^6$	$180.0 \pm 0.5$	$1.7938 \pm 0.0023$
15	$10^6$	$394 \pm 1$	$1.8395 \pm 0.0025$
17	$10^6$	$545 \pm 2$	$1.8595 \pm 0.0027$
21	$10^6$	$956 \pm 5$	$1.8944 \pm 0.0029$
23	$10^6$	$1219 \pm 7$	$1.9069 \pm 0.0030$
27	$10^6$	$1880 \pm 10$	$1.9328 \pm 0.0032$
29	$10^6$	$2270 \pm 20$	$1.9396 \pm 0.0032$
31	$10^6$	$2750 \pm 20$	$1.9549 \pm 0.0034$
35	$5 \times 10^5$	$3950 \pm 40$	$1.9810 \pm 0.0050$
41	$5 \times 10^5$	$6030 \pm 80$	$1.9967 \pm 0.0053$
51	$5 \times 10^5$	$11500 \pm 200$	$2.0398 \pm 0.0062$
61	$5 \times 10^5$	$19900 \pm 400$	$2.0744 \pm 0.0067$
71	$5 \times 10^5$	$29800 \pm 600$	$2.0830 \pm 0.0074$
81	$10^6$	$42800 \pm 700$	$2.0912 \pm 0.0060$
91	$5 \times 10^5$	$58000 \pm 1000$	$2.0960 \pm 0.0087$
101	$5 \times 10^5$	$76000 \pm 2000$	$2.0984 \pm 0.0092$
111	$5 \times 10^5$	$107000 \pm 3000$	$2.1295 \pm 0.0096$
121	$5 \times 10^5$	$154000 \pm 5000$	$2.1723 \pm 0.0107$

which are also directly measurable in the MC simulations. In other words, (3.23) and (3.24) can be expressed in the following way:

$$\frac{da(x)}{dx} = \frac{a(x)}{x} \langle N(x) \rangle, \quad (3.27)$$

$$\frac{d^2a(x)}{dx^2} = \frac{a(x)}{x^2} [\langle N(x)^2 \rangle - \langle N(x) \rangle]. \quad (3.28)$$

Therefore, we can obtain  $a(x^*)$  through the MC simulations, and, knowing  $\lambda_1$  from the preceding calculation of  $\nu$  (see Table II), we can apply (3.19) and (3.20) to learn  $\gamma$ . In Table III we present our MCRG results for  $\gamma$  for  $b > 9$ , as well as (for the sake of comparison with the exact results) for  $3 \leq b \leq 9$ . Hence one can see that the MCRG values deviate at most 0.06% from the available exact values.

The entire set of our results for  $\gamma$  is depicted in Fig. 7. First, we observe that all values of  $\gamma$  for the PF fractals are larger than the Euclidean value  $\gamma = 43/32$  [5], and, in addition, it appears that  $\gamma$  is a monotonically increasing function of  $b$ . Both findings are in accordance with the behavior of  $\gamma$  found for the first seven ( $2 \leq b \leq 8$ ) members of the SG family of fractals [13]. In the latter case, using the finite-size scaling arguments Dhar [25] found that  $\gamma$  should approach  $133/32$  when  $b \rightarrow \infty$ , with a negative correction term proportional to  $\ln \ln b / \ln b$ . In the case of the PF family of fractals, the same behavior of the spectral dimensions, for large  $b$ , for both families (SG and PF), and our present numerical findings, make us assume that  $\gamma$  continues to grow beyond  $\gamma = 2.1723$  (found for  $b = 121$ ) and approaches some finite value when  $b \rightarrow \infty$ . Indeed, if we follow the finite size scaling framework of Dhar [25], we find that the RG transformations for SAW's on the PF fractals have the same requisite structure exploited in the case of the SG fractals for large  $b$ . Next, if we use the data pertinent to the SAW criticality in the  $\pi/2$  wedge of the square lattice [26], we find that when  $b \rightarrow \infty$  the critical exponent  $\gamma$  for the PF fractals should approach the non-Euclidean value  $103/32$ .

The possible asymptotic behavior of the critical exponent  $\gamma$  for  $b > 121$  raises the question of the applicability of the MCRG method beyond the reached limit. As a matter of fact, the inset of Fig. 7 shows that our data for  $91 \leq b \leq 121$  do not display the smooth behavior of the kind that is observable in the case of data for  $b < 91$ . We have concluded that this fact can be related to the properties of the random number generator (RNG) used in the MC simulations. More specifically, we have used a portable multiple prime RNG [27] which provides 10 000 random numbers within the interval  $[0.0000, 0.9999]$ . However, Table II shows that the  $x^*$  data for  $b > 81$  are very densely distributed. Therefore, due to the fact that our MCRG calculations start with a given  $x$ , we need to perform more precise calculations in this region, and, to this end, we need a RNG that provides random numbers with at least five digits. Random numbers with eight digits can be obtained [27] by a concatenated use of the four-digit RNG, but this approach doubles the computation time. For instance, to calculate

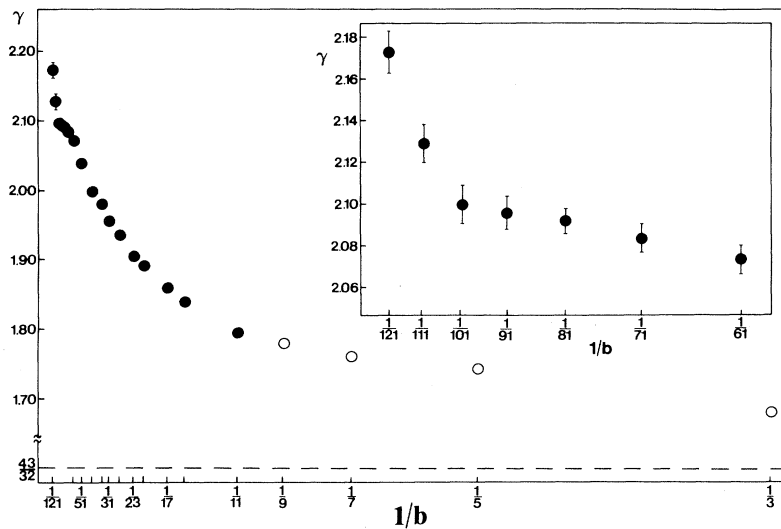


FIG. 7. The exact (open circles) and MCRG (solid circles) results for the critical exponent  $\gamma$  of SAW's on the PF fractals. In the inset, the last seven data ( $b \geq 61$ ) are depicted together with the corresponding error bars (the latter are hardly visible on the scale used for displaying all data). The horizontal dashed line represents the Euclidean value  $\gamma = 43/32$ .

in this way  $\gamma$  for  $b = 131$  (with  $5 \times 10^5$  MC simulations) it would take more than 11 days of continuous work of an IBM RS-6000 computer. For this reason, we did not extend our set of findings beyond  $b = 121$  [28].

#### IV. DISCUSSION AND SUMMARY

We have studied critical properties of SAW's on the infinite family of the PF fractals each member of which has the fractal dimension  $d_f$  equal to the Euclidean value 2, while their spectral dimensions  $d_s$  vary from 1.393 85 to 2 when the fractal enumerator  $b$  varies from 3 to  $\infty$ . In particular, we have calculated the SAW critical exponents  $\nu$  and  $\gamma$  via an exact RG (for  $3 \leq b \leq 9$ ) and via the MCRG approach (for  $b \leq 121$ ). Here we would like first to compare the obtained results for  $\nu$  with the corresponding phenomenological closed-form formulas. In this comparison, we skip the simplest formula  $\nu_F = 3/(2 + d_f)$  [29] since it erroneously predicts that  $\nu = 3/4$  for the entire PF family. In other words, we focus on those formulas for  $\nu$  that include the spectral dimension  $d_s$ . Chronologically, the first formula of interest

$$\nu_{RTV} = 3d_s/d_f(2 + d_s), \quad (4.1)$$

was proposed by Rammal, Toulouse, and Vannimenus [7]. Recently several groups of authors [8–11] obtained a formula which in the case of fractals studied here has the form

$$\nu_{HA} = (4d_f - d_s)/[d_f(2d_f - d_s + 2)]. \quad (4.2)$$

Finally, we quote the formula

$$\nu_{DMS} = (2d_f + d_s)/[d_f(2 + d_f)], \quad (4.3)$$

that was derived in Ref. [12]. In Fig. 8 we present comparison of our exact and MCRG results for  $\nu$  with the corresponding predictions that follow from formulas (4.1)–(4.3). One can see that all phenomenological formulas

wrongly predict behavior of  $\nu$  as a function of  $1/b$ . Noting that in the case under study the phenomenological formulas are functions of  $d_s$  only ( $d_f = 2$ , for all  $b$ ), we may conclude that the PF family of fractals provides a counterargument to the role given to the spectral dimension in the Flory-type approaches performed so far.

The data presented in Fig. 8 raise a question concerning the behavior of  $\nu$  when  $b \rightarrow \infty$ . The same question has been raised [13] and discussed [25] in the case of the SG family of fractals. Using the finite-size scaling arguments [25], it was predicted that  $\nu$  for SAW's on the SG fractals should approach the Euclidean value  $3/4$ , with a negative correction term of the type  $\ln \ln b / \ln b$ , when  $b$  tends to infinity. This asymptotic behavior, in combination with the exact results for  $\nu$  [13], implied a crossing of the Euclidean value  $3/4$  at some finite  $b$ , which was in fact confirmed in Ref. [14]. In the case of the PF fractals, we observe the same type of behavior of  $\nu$ , and, consequently, we can expect that  $\nu$  should also approach  $3/4$  from below, in the limit  $b \rightarrow \infty$  (this expectation can be corroborated by applying the finite-size scaling method of Dhar [25]). The established behavior of  $\nu$  up to  $b = 121$  (see Fig. 8) and the expected asymptotic behavior for large  $b$  imply that  $\nu$  has a minimum at some finite  $b$ . The location and physical meaning of this minimum are not clear at present. In fact, the minimum of  $\nu$  can be located [30] if one accepts the phenomenological assumption of Rammal, Toulouse, and Vannimenus [7] that the ratio  $\nu/\nu_{RW}$  is a certain function  $\phi$  of the spectral dimension  $d_s$ , where  $\nu_{RW} = d_s/2d_f$  is the random-walk critical exponent. Then, knowing that  $\phi$ , as a function of  $b$ , monotonically decreases from the value 2.274 22 for  $b = 3$  up to 1.760 96 for  $b = 121$ , and knowing its limiting value  $3/2$  (for  $b \rightarrow \infty$ ), one can [30] make a simple linear interpolation of  $\phi$  as a function of  $1/\ln b$  in the unknown region between  $b = 121$  and  $1/b = 0$ . In this way, one can learn that minimum of  $\nu$  occurs at  $b \approx 25\,000$ . However, it is not clear why one should assume the linear



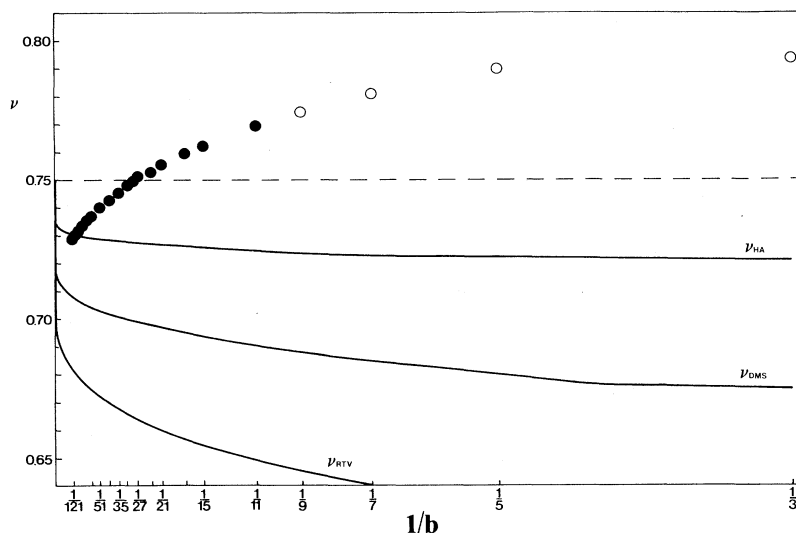


FIG. 8. The exact (open circles) and MCRG (solid circles) results for the critical exponent  $\nu$  of SAW's on the PF fractals. The error bars related to the MCRG results lie within the drawn circles (the size of the bars is at least seven times smaller than the diameter of the circles). The solid lines, marked by  $\nu_{HA}$ ,  $\nu_{DMS}$ , and  $\nu_{RTV}$ , show predictions that follow from the phenomenological formulas (4.2), (4.3), and (4.1), respectively. The horizontal dashed line represents the Euclidean value  $\nu = 3/4$ .

dependence of  $\phi$  of  $1/\ln b$ . For instance, if we make linear interpolation of  $\phi$  as a function of  $1/b$ , we find that the minimum of  $\nu$  occurs at  $b \approx 1800$ . In any case, both interpolations predict the location of minimum of  $\nu$  in the region that cannot be reached using the most powerful present day computers, and, accordingly, this problem remains open for future studies.

In this paper we have also reported on our exact ( $3 \leq b \leq 9$ ) and MCRG ( $b < 121$ ) calculations of the critical exponent  $\gamma$  for SAW's on the PF fractals. The calculation of  $\gamma$  through the MCRG method is, to our knowledge, the first such utilization of the method in the case of fractals. We have found that  $\gamma$  is a monotonically increasing function of the fractal enumerator  $b$  and for all studied cases of  $b$  it appears that  $\gamma$  is larger than the Euclidean value  $43/32$  [5]. These findings offer a specific support for the finite-size scaling predictions of the asymptotic behavior of  $\gamma$  [25] (invented originally for the SG family, whose  $\gamma$  is known only for the first seven fractals [13]). On the other hand, our results for  $\gamma$  are in disagreement with the various arguments [3,31] which state that  $\gamma$  for SAW's on the critical percolation clusters is not different from  $\gamma$  of SAW's on fully occupied Euclidean lattices. Of course, the PF fractals do not model the percolation clusters, and the observed disagreement may stem from the basic difference between deterministic and random fractals. Nevertheless, in view of the fact that the criticality of SAW's on the percolation clusters is still a controversial problem, the noted disagreement with our exact and MCRG results calls for further investigations.

#### ACKNOWLEDGMENTS

This work has been supported in part by the Yugoslav-USA Joint Scientific Board under Project No. JF900

(NSF), and by the Serbian Science Foundation under Project No. 0103. The authors would also like to acknowledge cordial help provided by Boriko Stošić in the computational part of this work. In addition, one of the authors (S.M.) would like to express his gratefulness to the Center for Polymer Studies and Department of Physics of the Boston University for the opportunity to use their computer facilities in the course of this work.

#### APPENDIX: COEFFICIENTS OF THE RG TRANSFORMATION

In this appendix we present coefficients of the RG transformations that have been used to calculate the critical exponents  $\nu$  and  $\gamma$  of the SAW's on the PF family of fractals. First, we give the coefficients  $a_N$  which appear in the RG relation (3.9):

$$b = 3$$

$$a_3 = 1, a_5 = 2;$$

$$b = 5$$

$$a_5 = 1, a_7 = 12, a_9 = 20, a_{11} = 12, a_{13} = 6, a_{15} = 2;$$

$$b = 7$$

$$a_7 = 1, a_9 = 30, a_{11} = 182, a_{13} = 440, a_{15} = 774, a_{17} = 1280, a_{19} = 1904, a_{21} = 2332, a_{23} = 1924, a_{25} = 826, a_{27} = 122;$$

$$b = 9$$

$$a_9 = 1, a_{11} = 56, a_{13} = 702, a_{15} = 3748, a_{17} = 12542, a_{19} = 35346, a_{21} = 93048, a_{23} = 231134, a_{25} = 538572, a_{27} = 1157132, a_{29} = 2193928, a_{31} = 3446672,$$

$a_{33} = 4\,232\,332$ ,  $a_{35} = 3\,860\,556$ ,  $a_{37} = 2\,478\,588$ ,  $a_{39} = 1\,042\,646$ ,  $a_{41} = 254\,744$ ,  $a_{43} = 27\,638$ ,  $a_{45} = 472$ .

In what follows we present the coefficients  $Q_N$  of the RG relation (3.21):

$b = 3$

$Q_1 = 3$ ,  $Q_2 = 5$ ,  $Q_3 = 4$ ,  $Q_4 = 8$ ,  $Q_5 = 2$ ,  $Q_6 = 2$ ;

$b = 5$

$Q_1 = 3$ ,  $Q_2 = 5$ ,  $Q_3 = 15$ ,  $Q_4 = 33$ ,  $Q_5 = 48$ ,  $Q_6 = 104$ ,  
 $Q_7 = 114$ ,  $Q_8 = 196$ ,  $Q_9 = 208$ ,  $Q_{10} = 250$ ,  $Q_{11} = 224$ ,  
 $Q_{12} = 186$ ,  $Q_{13} = 106$ ,  $Q_{14} = 56$ ,  $Q_{15} = 12$ ;

$b = 7$

$Q_1 = 3$ ,  $Q_2 = 5$ ,  $Q_3 = 15$ ,  $Q_4 = 33$ ,  $Q_5 = 87$ ,  
 $Q_6 = 201$ ,  $Q_7 = 398$ ,  $Q_8 = 900$ ,  $Q_9 = 1478$ ,  $Q_{10} = 3114$ ,  
 $Q_{11} = 4654$ ,  $Q_{12} = 8864$ ,  $Q_{13} = 12\,900$ ,  $Q_{14} = 21\,518$ ,  
 $Q_{15} = 30\,094$ ,  $Q_{16} = 43\,294$ ,  $Q_{17} = 54\,496$ ,  $Q_{18} = 68\,262$ ,

$Q_{19} = 72\,610$ ,  $Q_{20} = 78\,410$ ,  $Q_{21} = 68\,166$ ,  $Q_{22} = 59\,372$ ,  
 $Q_{23} = 41\,358$ ,  $Q_{24} = 25\,808$ ,  $Q_{25} = 13\,574$ ,  $Q_{26} = 5020$ ,  
 $Q_{27} = 1574$ ,  $Q_{28} = 184$ ;

$b = 9$

$Q_1 = 3$ ,  $Q_2 = 5$ ,  $Q_3 = 15$ ,  $Q_4 = 33$ ,  $Q_5 = 87$ ,  $Q_6 = 201$ ,  
 $Q_7 = 537$ ,  $Q_8 = 1261$ ,  $Q_9 = 2872$ ,  $Q_{10} = 6724$ ,  
 $Q_{11} = 13\,438$ ,  $Q_{12} = 30\,638$ ,  $Q_{13} = 56\,112$ ,  $Q_{14} = 122\,642$ ,  
 $Q_{15} = 214\,710$ ,  $Q_{16} = 445\,252$ ,  $Q_{17} = 764\,580$ ,  
 $Q_{18} = 1\,489\,630$ ,  $Q_{19} = 2\,507\,460$ ,  $Q_{20} = 4\,549\,028$ ,  
 $Q_{21} = 7\,396\,058$ ,  $Q_{22} = 12\,456\,940$ ,  $Q_{23} = 19\,188\,414$ ,  
 $Q_{24} = 30\,052\,712$ ,  $Q_{25} = 43\,067\,678$ ,  $Q_{26} = 62\,724\,968$ ,  
 $Q_{27} = 82\,429\,002$ ,  $Q_{28} = 110\,922\,050$ ,  $Q_{29} = 132\,313\,980$ ,  
 $Q_{30} = 162\,160\,674$ ,  $Q_{31} = 174\,252\,942$ ,  $Q_{32} = 190\,453\,060$ ,  
 $Q_{33} = 182\,794\,634$ ,  $Q_{34} = 173\,662\,376$ ,  
 $Q_{35} = 146\,726\,468$ ,  $Q_{36} = 117\,553\,854$ ,  $Q_{37} = 85\,103\,400$ ,  
 $Q_{38} = 55\,243\,168$ ,  $Q_{39} = 32\,659\,526$ ,  $Q_{40} = 16\,097\,526$ ,  
 $Q_{41} = 7\,109\,542$ ,  $Q_{42} = 2\,325\,828$ ,  $Q_{43} = 623\,048$ ,  
 $Q_{44} = 87\,742$ ,  $Q_{45} = 6614$ .

- 
- [1] C. Vanderzande and A. Komoda, Phys. Rev. A **45**, R5335 (1992).  
 [2] Y. Kim, Phys. Rev. A **45**, 6103 (1992).  
 [3] K. Y. Woo and S. B. Lee, Phys. Rev. A **44**, 999 (1991).  
 [4] P. Le Doussal and J. Machta, J. Stat. Phys. **64**, 541 (1991).  
 [5] B. Nienhuis, Phys. Rev. Lett. **49**, 1062 (1982).  
 [6] J. A. Given and B. B. Mandelbrot, J. Phys. B **16**, L565 (1983).  
 [7] R. Rammal, G. Toulouse, and J. Vannimenus, J. Phys. (Paris) **45**, 389 (1984).  
 [8] S. Havlin and D. Ben-Avraham, Adv. Phys. **36**, 695 (1987).  
 [9] A. Aharony and A. B. Harris, J. Stat. Phys. **59**, 1091 (1989).  
 [10] J. P. Bouchaud and A. Georges, Phys. Rev. B **39**, 2846 (1989).  
 [11] A. K. Roy and A. Blumen, J. Stat. Phys. **59**, 1581 (1990).  
 [12] R. Dekeyser, A. Maritan, and A. Stella, Phys. Rev. Lett. **58**, 1758 (1987).  
 [13] S. Elezović, M. Knežević, and S. Milošević, J. Phys. A **20**, 1215 (1987).  
 [14] S. Milošević and I. Živić, J. Phys. A **24**, L833 (1991).  
 [15] S. Milošević and I. Živić, Physica A **186**, 329 (1992).  
 [16] Z. Borjan, S. Elezović, M. Knežević, and S. Milošević, J. Phys. A **20**, L715 (1987).  
 [17] S. Milošević, D. Stassinopoulos, and H.E. Stanley, J. Phys. A **21**, 1477 (1988).  
 [18] For  $b > 41$ , ratios of some of the coefficients of the linear equations become larger than  $10^{15}$ , so that we could not use the available NDP FORTRAN-386 (even in the double-precision mode) installed on a computer with the Intel 80486 microprocessor. Thus, we have applied the MATHEMATICA software package which allowed us to find  $d_s$ , for  $b \leq 131$ , with arbitrary preset accuracy.  
 [19] D. Dhar, J. Phys. A **21**, 2261 (1988).  
 [20] D. Dhar, J. Math. Phys. **19**, 5 (1978).  
 [21] S. Redner and P. J. Reynolds, J. Phys. A **14**, L55 (1981).  
 [22] S. Redner and P. J. Reynolds, J. Phys. A **14**, 2679 (1981).  
 [23] There is no rigorous proof that the values of  $x^*$  given in Table II should converge to the value  $\mu^{-1} = 0379052$  found by A. J. Guttmann and I. G. Enting, J. Phys. A **21**, L165 (1988). However, the two recent studies of S. G. Whittington and A. J. Guttmann, J. Phys. A **23**, 5601 (1990), and T. W. Burkhardt and I. Guim, J. Phys. A **24**, L1221 (1991), which deal with SAW's that cross finite-size square lattices, provide solid grounds for expecting that  $x^*$  of Table II converge to  $\mu^{-1}$  when  $b \rightarrow \infty$ .  
 [24] S. Elezović-Hadžić, S. Milošević, H. W. Capel, and Th. Post, Physica A **179**, 39 (1991).  
 [25] D. Dhar, J. Phys. (Paris) **49**, 397 (1988).  
 [26] A. J. Guttmann and G. M. Torrie, J. Phys. A **17**, 3539 (1984); J. L. Cardy and S. Redner, *ibid.* **17**, L933 (1984).  
 [27] A. Haas, ACM Trans. Math. Software **13**, 368 (1987).  
 [28] In addition to the RNG from Ref. [27], we have tried the portable RNG's described in the book by W. H. Press, B. P. Flannery, S. A. Teukolsky, and W. T. Vetterling, *Numerical Recipes* (Cambridge University Press, Cambridge, 1989). However, the offered RNG's did not provide results of a reliability that was comparable with the reliability achieved by using RNG from Ref. [27].  
 [29] K. Kremer, Z.Phys. B **45**, 149 (1981); M. Sahimi, J. Phys. A **17**, L379 (1984).  
 [30] G. Huber (unpublished).  
 [31] J. W. Lyklema and K. Kremer, Z. Phys. B **55**, 61 (1984); S. B. Lee, H. Nakanishi, and Y. Kim, Phys. Rev. B **39**, 9561 (1989); P. M. Lam, J. Phys. A **23**, L831 (1990).